

# Radar Cross Section Reduction of Low Profile Fabry-Perot Resonator Antenna Using Checkerboard Artificial Magnetic Conductor

**Libi Mol Vadakkekallathil Abdul Hakim\* and Chandroth Karuvandi Aanandan**

<sup>1</sup>Department of Electronics, Cochin University of Science and Technology, Kerala, India

\*corresponding author, E-mail: libi.riyaz@gmail.com

## Abstract

This paper presents a novel low profile, high gain Fabry-Perot resonator antenna with reduced radar cross section (RCS). An artificial magnetic conductor which provides zero degree reflection phase at resonant frequency is used as the ground plane of the antenna to obtain the low profile behavior. A checkerboard structure consisting of two artificial magnetic conductor (AMC) surfaces with antiphase reflection property is used as the superstrate to reduce the RCS. The bottom surface of superstrate is perforated to act as partially reflective surface to enhance the directivity of antenna. The antenna has a 3 dB gain bandwidth from 9.32 GHz to 9.77 GHz with a peak gain of 12.95 dBi at 9.6 GHz. The cavity antenna also has reduced reflectivity with a maximum reduction of 14.5 dB at 9.63 GHz.

## 1. Introduction

The pioneering work of Fabry-Perot resonator antenna by G V Trentini [1] has found tremendous application in the design of highly directive planar antennas. It consists of a partially reflective surface (PRS) separated from ground plane to form an air filled cavity fed by antennas like dipole, printed patch or slot in the ground plane. In earlier studies different types of structures like 2D dielectric rods or grids [2], 3D electromagnetic band gap structures [3] were considered as PRS. One of the disadvantages of this configuration was narrow gain bandwidth. To overcome this, different methods were proposed in literature. In one of the methods [4], the slot antenna array with complex feeding network is used as the feed to obtain a bandwidth of 13.2%. Another method [5] proposes the use of PRS with positive reflection phase gradient as the superstrate for gain bandwidth improvement. Several PRS with this property are designed using 1D dielectric substrate, 2D frequency selective surfaces etc.

Artificial magnetic conductor introduced by Daniel Sievenpiper [6] attracted significant attention due to its in-phase reflection property at resonant frequency. The bandwidth of AMC is defined as the frequency range in which the reflection phase varies from  $+90^\circ$  to  $-90^\circ$ , because these phase values do not cause any destructive interference between direct and reflected waves. The AMC consists of a periodic array of patches over a grounded dielectric. AMC

has been used as the ground plane to design low profile cavity antennas with a directivity of 20.5 dBi and bandwidth 2% [7].

RCS is a measure of the detectability of a target when it is illuminated by electromagnetic field. Maurice Paquay [8] proposed in 2007 that the chessboard like combination of AMC cells with in-phase reflection property and metallic plate with  $180^\circ$  phase change can lead to destructive interference, resulting in a null in bore sight direction and hence a reduction in RCS. The main disadvantage of this configuration is its narrow bandwidth. The metal plate in chess board configuration is replaced by another AMC to obtain required phase difference ( $180^\circ \pm 30^\circ$ ) over a wider frequency range, resulting in broadband RCS reduction [9, 10]. Chess board AMC can be used as the ground plane [11] in planar antennas to reduce the RCS over a wide frequency range. A chess board AMC is designed to be used as the superstrate in cavity antenna for wideband structural RCS reduction with in-band reduction of 5.8 dB compared to feed antenna and it is reported that RCS reduction frequency range is not coinciding with phase difference [12].

In this paper, we investigate the use of AMC as ground plane as well as superstrate to design a low profile cavity antenna with reduced RCS. The square patch AMC having resonant frequency as that of the rectangular feed antenna is used as the ground plane to reduce the cavity height. Two different AMC elements with perforated ground [13] are arranged as chessboard to act as superstrate. The bottom surface shows partially reflecting characteristics which is the main requirement for a cavity superstrate to contribute for high directivity. In this proposed cavity antenna configuration, the checkerboard superstrate is backed by AMC ground plane at quarter wave distance. Since the AMC has variable reflection phase response from  $+180^\circ$  to  $-180^\circ$ , the RCS reduction performance of AMC checkerboard is quite different from that of free standing configuration. So the RCS reduction property of AMC elements are studied for both these configurations. It is noted that chessboard structure backed by AMC is providing required phase difference only for a narrowband, which results in narrowband RCS reduction.

## 2. Ray theory analysis of Fabry-Perot resonator antenna

The working principle of cavity antenna proposed in 1956 by G.V Trentini [1] is repeated here for the completeness of the analysis. The schematic of the antenna placed in front of the conducting plate and a partially reflective surface at a distance 'h' from the conducting plate is shown in figure 1 (a).

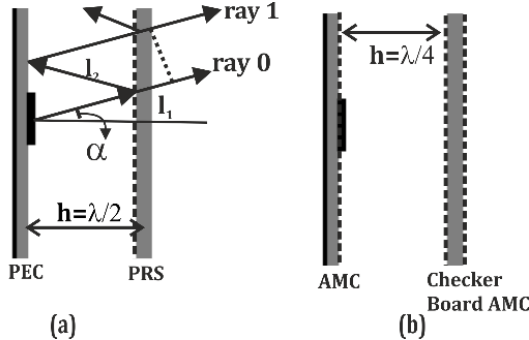


Figure.1. Configuration of cavity antenna (a) PEC ground plane (b) AMC ground plane

The radiation from the antenna is considered to be originating from a point with element pattern  $f(\alpha)$ . Due to the multiple reflection between the plates, the amplitude of ray 0 (the ray without any reflection) is proportional to  $\sqrt{1 - \rho^2}$ ; the magnitude of once reflected wave, ray 1 is proportional to  $\rho\sqrt{1 - \rho^2}$ ; etc., where  $\rho e^{j\varphi}$  is the reflection coefficient of the sheet. Assuming the sheet to be infinite in size and the maximum electric field from the antenna be  $E_0$ , the total electric field intensity in Fraunhofer region is given by-

$$E = \sum_{n=0}^{\infty} f(\alpha) E_0 \rho^n \sqrt{1 - \rho^2} e^{j\theta_n} \quad (1)$$

The phase angle  $\theta_n$  includes the phase variation due to the reflection from conducting plate ( $\delta$ ) and partially reflecting surface, path difference of transmitted rays and phase shift due to the transmission of rays through the partially reflecting surface, which is same for all the rays and is ignored in the calculation. The phase difference between ray n and ray 0 can be given as

$$\theta_n = n\phi = n \left[ -\frac{4\pi}{\lambda} h \cos \alpha - \delta + \varphi \right] \quad (2)$$

Since  $\rho < 1$ , the absolute value of field strength becomes

$$|E| = |E_0| f(\alpha) \sqrt{\frac{1 - \rho^2}{1 + \rho^2 - 2\rho \cos \phi}} \quad (3)$$

The height of the resonant cavity (h) to obtain the maximum power in broadside direction ( $\alpha=0$ ) can be derived from (3) and is given as-

$$h = \frac{\lambda}{4\pi} (2N\pi + \varphi - \delta), N = 0, 1, 2 \dots \quad (4)$$

The relative directivity of cavity antenna with respect to feed antenna can be given by-

$$D_r = 10 \log \frac{1 + \rho}{1 - \rho} \quad (5)$$

If the antenna is operating at first resonant frequency and the reflection phase of the PRS ( $\varphi$ ) =  $\pi$ , the height of the cavity antenna can be calculated as half the wavelength.

If the conducting ground plate is replaced by an artificial magnetic conductor with reflection phase variation

from  $+\pi$  to  $-\pi$  as shown in Fig.1 (b), the height of the resonant cavity to obtain the maximum power in broadside direction should be  $0 \leq h \leq \frac{\lambda}{2}$ . Therefore, AMC having resonant frequency same as that of the fundamental resonant frequency of the cavity antenna can be used as the ground plane to obtain the low profile cavity antenna.

### 3. Design of Feed antenna with AMC Ground plane

#### 3.1. Design of AMC ground plane

AMC ground plane is designed by using frequency domain solver in CST MW Studio. The unit cell consist of square patch over RT Duroid substrate having thickness  $h_1 = 0.8$  mm and dielectric constant 2.2, as shown in figure 2 (a). The reflection coefficient magnitude and phase obtained by simulation is depicted in figure 2 (b). The results shows that the resonant frequency is at 9.516 GHz with bandwidth of operation from 8.95 GHz to 10.05 GHz and the reflection coefficient magnitude is approximately 1.

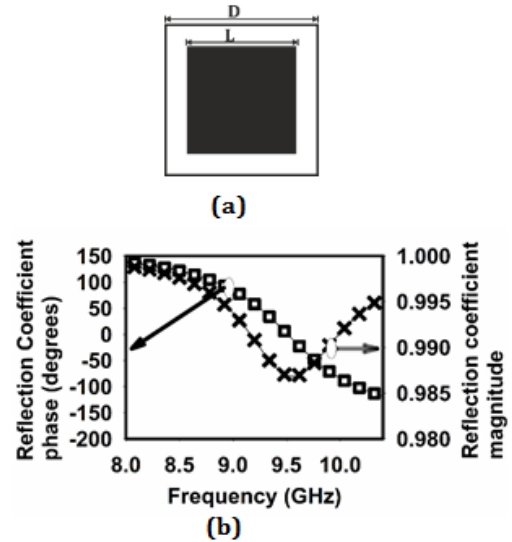


Figure.2. AMC ground plane (a) unit cell ( $D = 11.5$  mm and  $L = 9.3$  mm) (b) Simulated reflection characteristics

#### 3.2. Design of feed antenna with AMC ground

A microstrip patch antenna excited by a coaxial probe resonating at 9.55 GHz is used as the feed in cavity antenna. The patch antenna of dimensions 9.4 mm x 10.5 mm and the AMC patches are arranged on a metal backed substrate with dimensions of 100 mm x 100 mm. The antenna is fed by coaxial probe at 2 mm offset from the center. Some distance of separation between the antenna and AMC patch is maintained in all the sides for better matching. The matching of the antenna is get worsened when the distance of separation between the two decreases. Also, when the AMC is placed at large distance from the antenna, the performance of the cavity antenna get deteriorated as it is acting as PEC ground plane near to antenna and AMC ground in rest of the area. CST MW

Studio is used for the optimization of the distance of separation between the antenna and AMC patch. The prototype of fabricated feed antenna is given in figure 3 (a). The response of the antenna with AMC ground plane is shown in figure 3 (b), which shows matching from 9.48 GHz to 9.97 GHz.

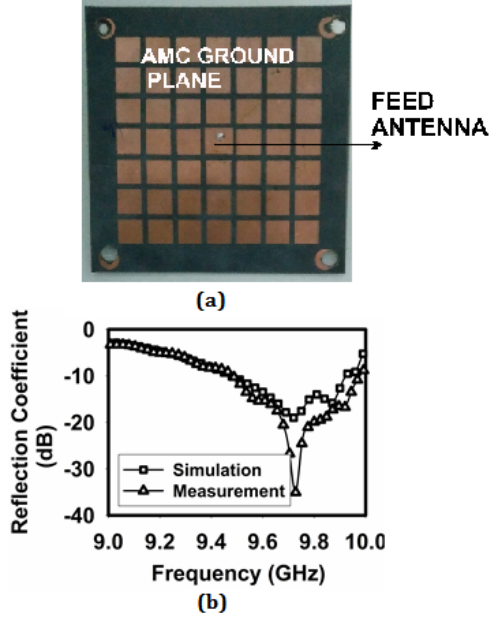


Figure.3. Feed antenna (a) Fabricated prototype (b) Simulated and measured response

#### 4. Design strategy for Checkerboard Surfaces to act as Superstrate

To design checkerboard surfaces to act as superstrate in cavity antennas to reduce the RCS and to enhance the gain, two conditions should be satisfied: the first is to obtain the  $180^\circ$  phase difference between the two structures to cancel out the scattered field and thus to satisfy the RCS reduction requirement and the second is to obtain the partially reflecting phase response from the bottom surface. The geometry of the designed structure and the response from top and bottom surface is discussed below.

The unit cells of checkerboard surface consist of two AMC unit cells: AMC-I and AMC-II as shown in figure 4 (a) and (b). Both of them are square patch with different dimensions. They are located on the top of FR4 substrate with dielectric constant of 4.4 and thickness of 0.8 mm. The bottom portion of substrate has perforations as in figure 4(c). The unit cell dimensions, of AMC-I and AMC-II, are taken same to include the integer number of cells in checkerboard structure. The number of AMC elements is optimized by simulation. It is observed that when the number of elements is less than four, the reflection characteristics are not satisfactory while more than four elements results in large structures. So four units of each AMC-I and AMC-II cells are alternatively placed to form a chessboard structure unit with resulting dimensions of  $40 \times 40 \text{ mm}^2$ . The fabricated

prototype of the structure consisting of  $2 \times 2$  array of unit cell is shown in figure 4 (d) and (e).

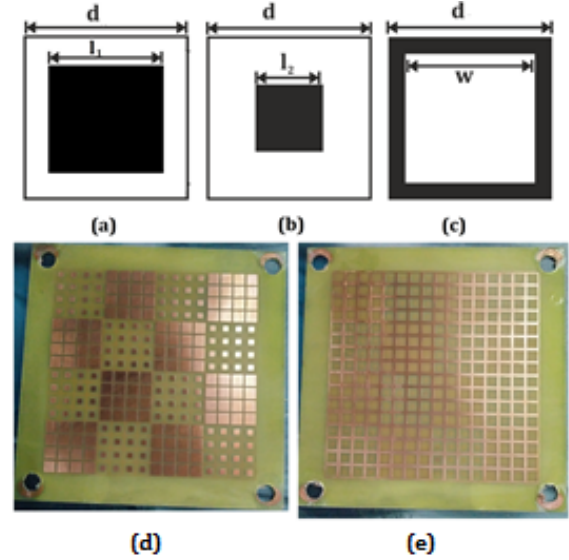


Figure.4. Superstrate structure details (a) AMC-unit cell I (top) (b) AMC- unit cell II (top) (c) AMCs unit cell (bottom) (d) fabricated prototype top view (e) bottom view ( $d= 5 \text{ mm}$ ,  $l_1= 4.1 \text{ mm}$ ,  $l_2= 2 \text{ mm}$ ,  $w= 4 \text{ mm}$ )

At first, the reflection characteristics of the bottom surface excited by an electromagnetic wave is analyzed. The unit cell boundary condition is employed here to reduce the computation time. The simulated reflection coefficient phase and magnitude is depicted in figure 5. The reflection coefficient magnitude is greater than 0.5 and phase is showing a positive gradient within the frequency range from 9.4 GHz to 9.8 GHz, which are the main requirements for a structure to act as superstrate in cavity antennas. The minimum magnitude is shown at 9.6 GHz.

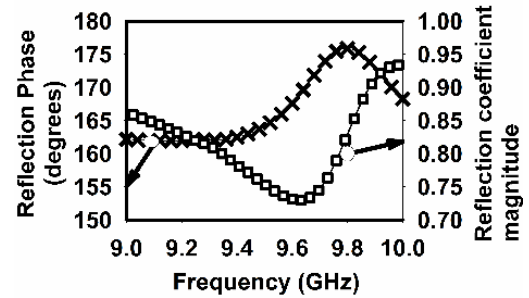


Figure.5. Simulated response from bottom surface of checkerboard unit cell

To study the characteristics of the top surface, the phase response from free standing AMC-I, AMC-II are simulated and shown in figure 6 (a). The phase difference satisfies  $180^\circ \pm 30^\circ$  from 10.1 GHz to 11.3 GHz. The RCS reduction of checkerboard surface compared to that of PEC is calculated as-

$$\text{RCS reduction} = 10 \log \left[ \frac{M_1 e^{jP_1} + M_2 e^{jP_2}}{2} \right]^2 \quad (6)$$

Where  $M_1$  and  $M_2$  are the reflection coefficient magnitude and  $P_1$  and  $P_2$  are the reflection phase of AMC-I and AMC-II.

II, respectively [10]. The calculated value shown in figure 6 (b) indicates that the free standing checkerboard structure can provide 10 dB RCS reduction from 10 GHz to 12 GHz.

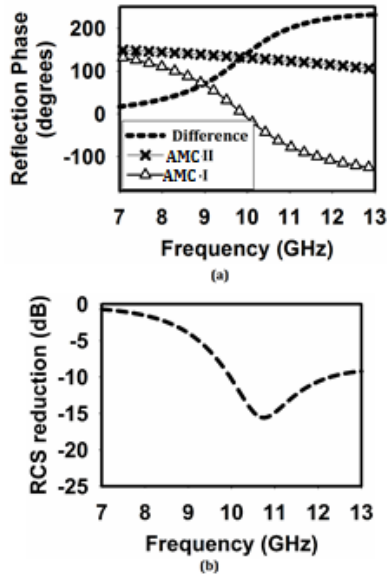


Figure.6.Simulated response from top surface of free standing checkerboard (a) Reflection phase characteristics (b) calculated RCS reduction

Here, the checkerboard is backed by AMC ground at quarter wave distance in cavity antenna. The reflection phase characteristics and calculated RCS reduction for this configuration are plotted in figure 7 (a) and (b). This configuration satisfies  $180^\circ \pm 30^\circ$  from 9.5 GHz to 9.8 GHz and it exhibits 10 dB RCS reduction over a narrow frequency range from 9.4 GHz to 9.8 GHz. The maximum RCS reduction occurs at 9.62 GHz, where the phase difference is  $180^\circ$ .

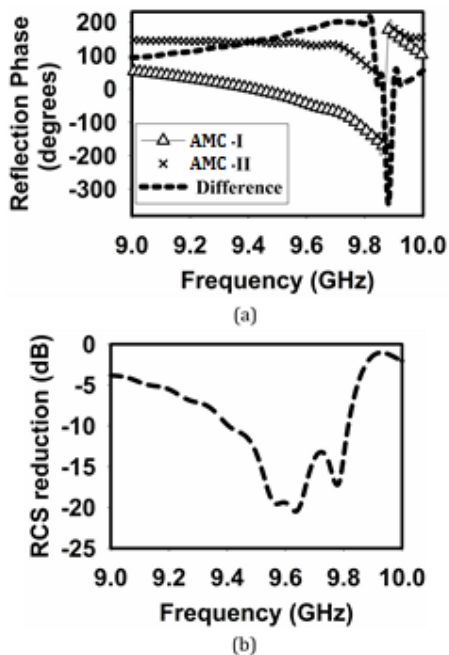


Figure.7. Simulated response from chessboard structure with AMC ground plane (a) Reflection phase characteristics (b) calculated RCS reduction

## 5. Proposed cavity antenna-fabrication and measurement

Fabricated prototype of the cavity antenna and its response is shown in figure 8. (a) and (b), respectively. The superstrate is suspended above the feed antenna using nylon spacers. The total dimension of the antenna is taken as 100 mm \* 100 mm to attach the spacers. The height of the resonant cavity (h) to obtain the maximum power in broadside direction is calculated using equation (4) and it is 7.8 mm at the resonant frequency (9.6 GHz), which is half of that with metal ground plane.

The measured result shows that the cavity antenna works with  $S_{11}$  below -10 dB from 9.33 GHz to 9.89 GHz. The simulated result shows bandwidth from 9.5 GHz to 9.88 GHz. The small difference may be caused by the presence of nylon spacers or the bending of superstrate due to the absence of spacers at the centre, which were not considered during simulation.

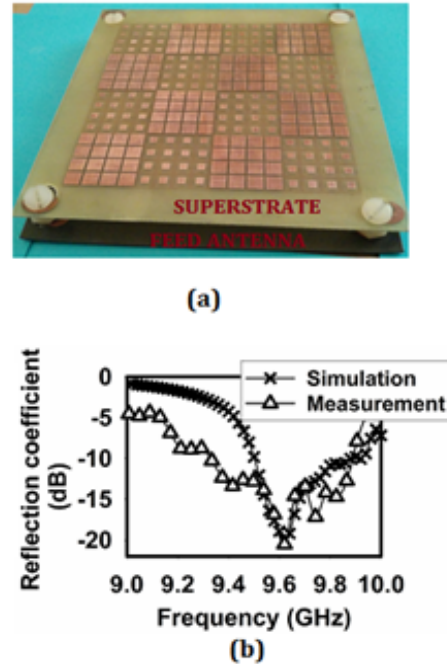


Figure.8. (a) Fabricated prototype of cavity antenna (b) Antenna response

The simulated directivity of feed and cavity antenna is presented in figure 9 (a). Assuming the size of PRS as infinite, the relative directivity of cavity antenna with respect to feed antenna can be calculated by using equation (5). At the resonant frequency  $\rho$  is 0.7315 and the relative directivity can be calculated as 8.095 dBi. The directivity of feed antenna at resonance is 7.45 dBi. Hence the total directivity of cavity antenna is 15.53 dBi. The directivity of cavity antenna obtained by simulation is 12.95



dBi. The difference in simulated and calculated directivity may be due to the finite size of PRS. By employing more number of checkerboard unit cells on the superstrate, the directivity of cavity antenna can be improved. The 3 dB gain bandwidth is 2.6%, from 9.49 GHz to 9.74 GHz.

The gains of the antennas are measured by gain comparison method and is shown in figure 9 (b). The maximum gain of feed antenna is measured as 4.6 dBi and it is 10.5 dBi for cavity antenna.

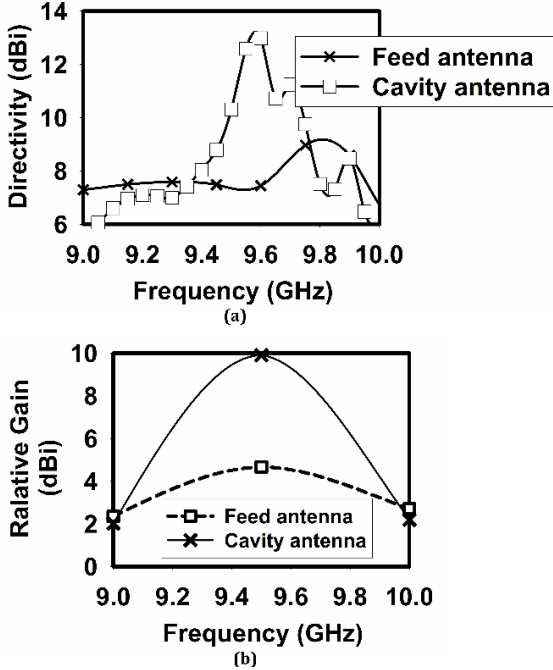


Figure.9. (a) Simulated directivity (b) Measured antenna gain

The efficiency of antenna is measured and the result is depicted in figure 10. It indicates that the efficiency of cavity antenna is less than that of the feed antenna, which can be accounted for additional loss in the superstrate. The cavity antenna has peak efficiency of 85.75% at 9.65 GHz.

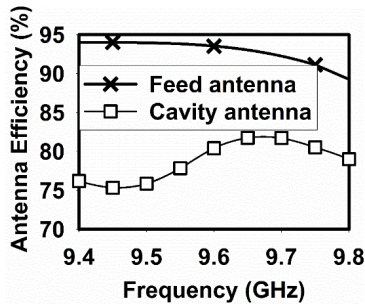


Figure.10. Measured Efficiency

To validate the RCS reduction of cavity antenna, reflected powers from the feed antenna and cavity antenna are measured in an anechoic environment and the photograph of the measurement set up is given in figure 11.

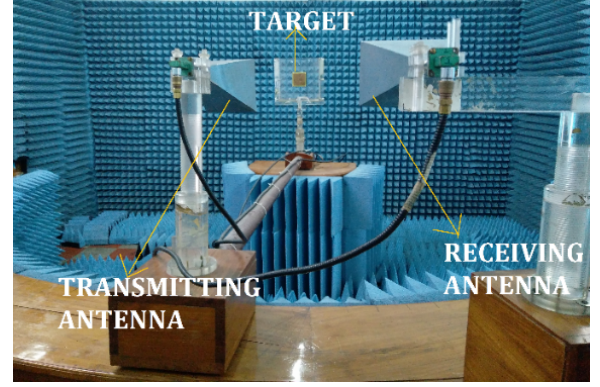


Figure.11. RCS Measurement Set up (Both the antennas are held apart to obtain the exact view of set-up)

RCS reduction characteristics were studied for both horizontal and vertical polarized incident wave and is depicted in figure 12 (a). The reflected power from the metal plate is normalized to cancel out the cable loss. Within the operating frequency range, the reflected power from the cavity antenna is 5 dB less than that from feed antenna. The maximum reduction in reflectivity (-14.5 dB) is observed at 9.63 GHz for horizontal polarized incident wave. Due to the symmetry of the structure, same response is also expected for vertical polarized wave. But the variation in response can be accounted for the slight misalignment of unit cell in different directions while fabrication. The RCS reduction characteristics of chessboard superstrate also depends on the angle of incidence. So the effect of oblique incidence is also studied for both horizontal and vertical polarization and the reflected power (bistatic RCS) with respect to the feed antenna response are shown in figure 12 (b). As the angle of incidence increases, the bistatic RCS reduction performance of the structure is deteriorating for both polarizations. The monostatic RCS will be very small for oblique incidence since the structure is planar.

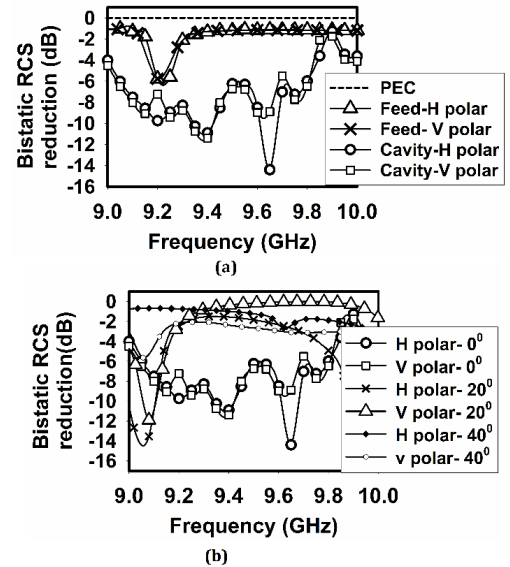


Figure.12. RCS reduction for (a) normal incidence (b) oblique incidence

The measured and simulated radiation pattern in E and H planes for the resonant frequency of 9.6 GHz are shown in figure 13 (a) and (b), respectively. Good agreement between measurements and simulations are observed. The cross polarization level is less than -15 dB in both planes. The high side lobe level (-10 dB) is due to the smaller aperture dimension of the antenna ( $2.5 \lambda$ ) [16].

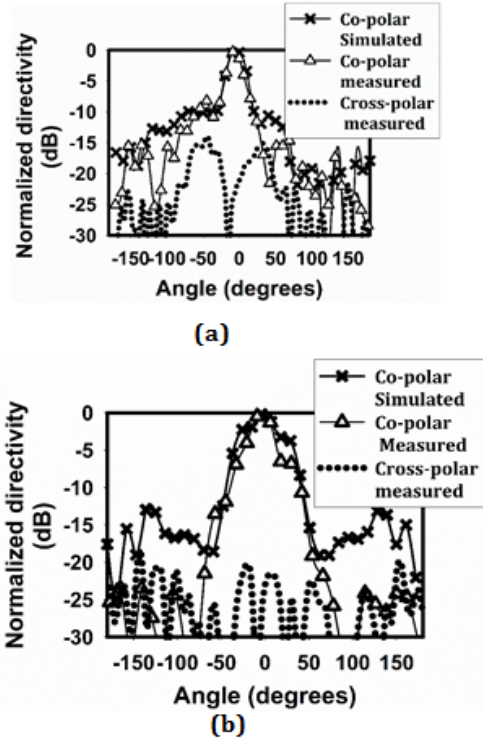


Figure.13. Radiation pattern of cavity antenna at 9.6 GHz  
(a) E-plane (b) H-plane

Table I: Comparison with other cavity antennas

Ref	Operation Frequency (GHz)	Max gain	Gain Enhancement (dB)	3-dB bandwidth (%)	Cavity height	In band RCS Reduction
[7]	14	20.5 dBi (directivity)	Not specified	2	5.9 ( $\lambda/3.63$ )	No
[12]	9.6	13.2 dBi	4.8	14.3	16 ( $\lambda/1.95$ )	Yes (5.8 dB)
[14]	11.5	13.2 dBi	6.5	3.6	9.95 ( $\lambda/2.62$ )	Yes (3 dB)
[15]	7.65	12.3 dB	4.6	11.07	22 ( $\lambda/1.78$ )	Yes (25 dB)
Proposed	9.6	10.5 dBi	5.9	2.6	7.8 ( $\lambda/4$ )	Yes (7.2 dB)

## References

1. Trentini, G.V, Partially reflecting sheet arrays, *IRE Trans. Antennas Propag.*, vol. 4, no. 4, pp. 666–671, Oct. 1956.
2. Y. J. Lee, J. Yeo, R. Mittra, and S. P. Wee, Application of electromagnetic bandgap (EBG) superstrates with controllable defects for a class of patch antennas as spatial angular filters, *IEEE Trans. Antennas Propag.*, vol. 53, no. 1, pp. 224–235, Jan. 2005.

Table I shows a comparison between the proposed antenna and recently reported Fabry-perot cavity antennas. The proposed cavity antenna offers a more compact design with in band RCS reduction.

## 6. Conclusion

A low profile high gain Fabry-Perot cavity antenna with RCS reduction is presented. The height of the cavity antenna is reduced by half by the application of artificial magnetic conductor as the ground plane of feed antenna. By employing the checkerboard AMC with perforated ground as the superstrate, the proposed antenna achieved RCS reduction and gain enhancement simultaneously. The antenna provides 3 dB gain bandwidth from 9.32 GHz to 9.77 GHz with a peak gain of 12.95 dBi at 9.6 GHz. The maximum reduction in reflectivity (-14.5 dB) is achieved at 9.63 GHz for horizontal polarized wave incidence and RCS reduction of 7.2 dB is achieved at 9.6 GHz. A prototype of the structure is fabricated and the measured results agree well with simulations. The proposed cavity antenna offers gain enhancement and RCS reduction with optimum thickness.

## Acknowledgement

Authors would like to acknowledge the financial and infrastructural support from University Grants Commission and Department of Science and Technology, Government of India. The authors also like to express gratitude to Rogers Corporation for supplying substrate by University Sample Program.

3. Y. Lee, X. Lu, Y. Hao, S. Yang, J. Evans, and C. G. Parini, Low-profile directive millimeter-wave antennas using free-formed three-dimensional (3-D) electromagnetic bandgap structures, *IEEE Trans. Antennas Propag.*, vol. 57, no. 10, pp. 2893–2903, Oct. 2009.
4. A. Weily, K. P. Esselle, T. S. Bird, and B. C. Sanders, Dual resonator 1-D EBG antenna with slot array feed for improved radiation bandwidth, *IET Microwaves*,

- Antennas Propag.*, vol. 1, no. 1, pp. 198–203, Feb. 2007.
5. A. P. Feresidis and J. C. Vardaxoglou, High gain planar antenna using optimized partially reflective surfaces, *IEEE Proc. Microwaves, Antennas Propag.*, vol. 148, no. 6, pp. 345–350, Dec. 2001.
  6. Sievenpiper, D., Zhang, L., Broas, R.F.J., Alexopoulos, N.G., and Yablonovitch, E., High-impedance electromagnetic surfaces with a forbidden frequency band, *IEEE Trans. Microw. Theory Tech.*, vol. 47, no. 11, pp. 2059–2074, Nov. 1999.
  7. S.Wang, A.P.Feresidis, G. Goussetis and J.C. Vardaxoglou, Low-profile resonant cavity antenna with artificial magnetic conductor ground plane, *Electron. Lett.* vol. 40, no.7, pp. 405-406, Apr. 2004.
  8. Maurice Paquay, Juan-Carlos Iriarte, Inigo Ederra, Ramon Gonzalo and Peter de Maagt, Thin AMC structure for Radar Cross-Section Reduction, *IEE Tran. Antennas and Prop*, vol. 55, no. 12, pp. 3630-3638, Dec. 2007
  9. Juan Carlos Iriarte Galarregui, Amagoia Tellechea Pereda, Jose Luis Martinez De Falcon, Inigo Ederra, Ramon Gonzalo and Peter de Maagt, Broad band Radar Cross Section Reduction Using AMC Technology, *IEEE Trans. Antennas and Prop*, vol. 61, no. 12, pp. 6136-6143, Dec. 2013
  10. Wengang Chen, Constantine A Balanis and Craig.R Birtcher, CheckerBoard EBG Surfaces for Wideband radar Cross Section Reduction, *IEEE Trans. Antennas and Prop*, vol. 63, no. 6, pp. 2636-2645, Jun. 2015.
  11. Yue-jun Zheng, Jun Gao, Xiang-yu Cao, Zidong Yuan, and Huanhuan Yang, Wideband RCS Reduction of a Microstrip Antenna Using Artificial Magnetic Conductor Structures, *IEEE Antennas and Wireless Propagation Letters*, vol. 14, pp. 1582-1585, Mar. 2015
  12. Yue-jun Zheng, Jun Gao, Xiang-yu Cao, Si-jia Li and Wen-qiang Li, Wideband RCS reduction and gain enhancement microstrip antenna using chessboard configuration Superstrate, *Microwave and Optical Technology Letters*, vol. 57, no.7, pp. 1738-1741, Jul. 2015.
  13. A. C. Durgun, C. A. Balanis, C. R. Birtcher, H. Huang and H. Yu, High-Impedance Surfaces With Periodically Perforated Ground Planes, *IEEE Transactions on Antennas and Propagation*, vol. 62, no. 9, pp. 4510-4517, Sept. 2014.
  14. W. Pan, C. Huang, P. Chen, X. Ma, C. Hu and X. Luo, A Low-RCS and High-Gain Partially Reflecting Surface Antenna, *IEEE Transactions on Antennas and Propagation*, vol. 62, no.2, pp.945-949, Feb. 2014.
  15. J. Mu, H. Wang, H. Wang and Y. Huang, Low-RCS and Gain Enhancement Design of a Novel Partially Reflecting and Absorbing Surface Antenna, *IEEE Antennas and Wireless Propagation Letters*, vol. 16, no. , pp. 1903-1906, 2017.